

Effect of grain boundary energy anisotropy on grain growth in ZK60 alloy using a 3D phase-field modeling

Yu-Hao Song(宋宇豪)[1], Ming-Tao Wang(王明涛)[1, 2, 3, †], Jia Ni(倪佳)[1], Jian-Feng Jin(金剑锋)[1, 2], and Ya-Ping Zong(宗亚平)[1]

Citation: Chin. Phys. B, 2020, 29 (**12**): 128201. DOI: 10.1088/1674-1056/abad1f
Journal homepage: http://cpb.iphy.ac.cn; http://iopscience.iop.org/cpb

What follows is a list of articles you may be interested in

Distribution of a polymer chain between two interconnected spherical cavities

Chao Wang(王超), Ying-Cai Chen(陈英才), Shuang Zhang(张爽), Hang-Kai Qi(齐航凯), Meng-Bo Luo(罗孟波)
Chin. Phys. B, 2020, 29 (**10**): 108201. DOI: 10.1088/1674-1056/abaedc

The n-type Si-based materials applied on the front surface of IBC-SHJ solar cells

Jianhui Bao(包建辉), Ke Tao(陶科), Yiren Lin(林苡任), Rui Jia(贾锐), Aimin Liu(刘爱民)
Chin. Phys. B, 2019, 28 (**9**): 098201. DOI: 10.1088/1674-1056/ab33ec

Effect of elastic strain energy on grain growth and texture in AZ31 magnesium alloy by phase-field simulation

Ri He(何日), Ming-Tao Wang(王明涛), Jian-Feng Jin(金剑锋), Ya-Ping Zong(宗亚平)
Chin. Phys. B, 2017, 26 (**12**): 128201. DOI: 10.1088/1674-1056/26/12/128201

Diffusion in the aged aluminium film on iron

A Y Galashev, O R Rakhmanova, V A Kovrov, Yu P Zaikov
Chin. Phys. B, 2017, 26 (**3**): 038201. DOI: 10.1088/1674-1056/26/3/038201

Modeling the temperature-dependent peptide vibrational spectra based on implicit-solvent model and enhance sampling technique

Tianmin Wu (吴天敏), Tianjun Wang (王天骏), Xian Chen(陈娴), Bin Fang(方彬), Ruiting Zhang(张睿挺), Wei Zhuang(庄巍)
Chin. Phys. B, 2016, 25 (**1**): 018201. DOI: 10.1088/1674-1056/25/1/018201

Effect of grain boundary energy anisotropy on grain growth in ZK60 alloy using a 3D phase-field modeling*

Yu-Hao Song(宋宇豪)[1], Ming-Tao Wang(王明涛)[1,2,3,†], Jia Ni(倪佳)[1], Jian-Feng Jin(金剑锋)[1,2], and Ya-Ping Zong(宗亚平)[1]

[1] *School of Materials Science and Engineering, Northeastern University, Shenyang* 110819, *China*
[2] *State Key Laboratory of Rolling and Automation, Northeastern University, Shenyang* 110819, *China*
[3] *Research Centre for Metallic Wires, Northeastern University, Shenyang* 110819, *China*

(Received 21 May 2020; revised manuscript received 1 July 2020; accepted manuscript online 7 August 2020)

A three-dimensional (3D) multiple phase field model, which takes into account the grain boundary (GB) energy anisotropy caused by texture, is established based on real grain orientations and Read–Shockley model. The model is applied to the grain growth process of polycrystalline Mg (ZK60) alloy to investigate the evolution characteristics in different systems with varying proportions of low-angle grain boundary (LAGB) caused by different texture levels. It is found that the GB energy anisotropy can cause the grain growth kinetics to change, namely, higher texture levels (also means higher LAGB proportion) result in lower kinetics, and *vice versa*. The simulation results also show that the topological characteristics, such as LAGB proportion and distribution of grain size, undergo different evolution characteristics in different systems, and a more serious grain size fluctuation can be caused by a higher texture level. The mechanism is mainly the slower evolution of textured grains in their accumulation area and the faster coarsening rate of non-textured grains. Therefore, weakening the texture level is an effective way for implementing a desired homogenized microstructure in ZK60 Mg alloy. The rules revealed by the simulation results should be of great significance for revealing how the GB anisotropy affects the evolution of polycrystalline during the grain growth after recrystallization and offer the ideas for processing the alloy and optimizing the microstructure.

Keywords: phase-field model, grain boundary (GB) energy anisotropy, grain size fluctuation, ZK60 alloy

PACS: 82.20.Wt, 81.10.–h, 91.60.Ed, 68.55.jm **DOI:** 10.1088/1674-1056/abad1f

1. Introduction

A strong deformation texture such as fiber texture after extrusion[1,2] and sheet texture after rolling[3,4] could be easily formed in the deformation process due to its limited slip system in Mg alloy. Subsequently, annealing texture forms at elevated temperature in the dynamic/static recrystallization process and coarsening process.[5,6] In general, texture is very common in Mg alloys and plays an important role especially in coarsening process in which the GB energy is the main driving force after the distortion energy has exhausted. The essential coarsening process is GBs' movement. Hence, the microstructure evolution is largely affected by the GB energy with an anisotropic feature caused by crystal orientation in a real alloy. Therefore, the effect of texture level plays an important role during morphological evolution. And it is necessary to study the effect of anisotropic GB energy in polycrystalline systems with varying texture levels during coarsening. However, it is difficult and costly to perform a quantitative research by an experimental method due to the influence of disturbing factors and the difficulty in controlling the orientation in a system with massive grains. Computational simulation is an effective way, which can study microstructure evolution, such as grain growth,[7–9] texture evolution,[10,11] and precipitation,[12–15] and also predict thermomechanical response during processing.[16,17]

Owing to its advantages such as simulating microstructure on a mesoscopic scale and avoiding tracking the interface explicitly, the phase field model is widely used for crystal evolution.[18–23] Meanwhile the effect of anisotropy caused by the GB energy depending on the neighboring grains dihedral angle can be revealed by the phase field simulation. There are some models proposed to investigate the effect of GB energy anisotropy on microstructures in two dimensions, which are mainly limited by the computational resources. Suwa and Saito[24] simulated the microstructure in a polycrystalline system by modifying parameters related to the GB energy in the model. They also came up with a concept of microstructural entropy to analyze the microstructure features such as the distribution of grain sizes and edges quantitively. Abrivard *et al.*[25] studied the effect of curvature, mobility and microrotation of GBs on the evolution in Al polycrystalline system and found that the simulation data and the experimental results

*Project supported by the National Key Research and Development Program of China (Grant No. 2016YFB0701204), the 111 Project, China (Grant No. B20029), the Fundamental Research Funds for the Central Universities, China (Grant Nos. N2002017 and N2007011), the National Natural Science Foundation of China (Grant No. 51571055), and the Science Fund from the Science and Technology Bureau of Jiangyin High-Tech Industrial Development Zone, China (Grant No. ZX20200062).

†Corresponding author. E-mail: wangmingtao@mail.neu.edu.cn

© 2020 Chinese Physical Society and IOP Publishing Ltd

are in good agreement with each other. Zaeem *et al.*[26] and Mallick and Vedantam[27] introduced a Read–Shockley model into a phase-field model for anisotropic GBs caused by adjacent grains microrotation to investigate morphological features. Miyoshi and Takaki[28] improved the accuracy of phase field model[29,30] by considering the anisotropic GB features and performed the simulation of abnormal grain growth in a polycrystalline system. They[31] also obtained statistically and numerically reliable results during anisotropic evolution in a two-dimensional (2D) large grain system. Vuppuluri and Vedantam[32] studied the microstructure controlled by the GB migration and grain rotation through using a model considering the anisotropic GB energy. Recently, Shahnooshi *et al.*[23] investigated the effect of anisotropic grain boundary energy on the kinetics of stressed grain growth by a 2D phase field model.

However, the spatial dimension is an important factor affecting the morphology and growth dynamics of microstructure. With the improvement of computing technology, more simulations are performed in 3D conditions so that the revealed evolutionary mechanism accords well with the real process. Mckenna *et al.*[33] investigated the effect of boundary thickness, triple junctions, misorientation, and anisotropy in the 2D case and built a double-crystal model in a 3D case to test the effects of misorientation and anisotropy, however, the model is not extended to a polycrystalline system including collective grains' behavior because of computational resources limitation. Suwa *et al.*[34] created an anisotropic 3D model including two types of textures by modifying the algorithm of dynamic grain-orientation reassignment proposed by Krill and Chen.[35] Similarly, Chang *et al.*[36] investigated the microstructure features affected by the uniform GB energy between two phases. However, the GB dihedral angle is not determined by the real orientation of adjacent grains but phenomenological variables. Kim *et al.*[37] proposed a 3D phase-field model combined with a GB energy database in pure Fe (0 K) and compared the effects among different GB conditions (isotropy and anisotropy).

However, most of the models are not suitable for real alloys due to a lack of valid system information.[24,26–28] The purpose of this paper is to build a 3D phase field model, which takes the GB energy anisotropy into account, and study the effect of GB energy anisotropy on grain growth kinetics and topology in a real ZK60 alloy. We introduce real orientation information represented by Euler angles into our model so that the real dihedral angle between adjacent grains can be determined. Also the active parameter tracking (APT) algorithm is employed so that a 3D simulation can be completed under current computing power. Then the relationship between model parameters and GB energy, which are both related to dihedral angle, can be established based on the Read–Shockley model by the numerical fitting. Finally the model is applied to a ZK60 Mg alloy with parameters cited from our previous work,[38] and the effects of GB energy anisotropy on growth kinetics and morphology features, including the distribution of grain size, grain size fluctuation, *etc*., will be investigated.

2. Phase-field model

2.1. Multi-order parameter phase field model

The primary purpose of this study is to investigate the influence of GB energy anisotropy on the coarsening process after recrystallization in a polycrystalline system. A modified polycrystalline phase field model, considering the anisotropy of GB energy based on real dihedral angle between adjacent grains, is proposed. Basically, a polycrystalline system can be described by a set of order variables $(\eta_i(r,t),\ i=1,2,\ldots n)$, which are the continuous functions in time and space dimensions in normal grain growth phase field model.[19,39] In order to describe the real dihedral angle between adjacent grains with different orientations, a set of orientation variables expressed in terms of Euler angles $(\alpha_i(\varphi_1\phi\varphi_2 rt), \varphi_1\in(0,2\pi), \phi\in(0,\pi), \varphi_2\in(0,2\pi))$ is introduced into our model. The order variables and orientation variables are separate information and connected by the index i in each simulated grid, namely, η_i represents the i-th grain's order variable value and $\alpha_i^{\varphi_1}$, α_i^{ϕ}, $\alpha_i^{\varphi_2}$ refer to the Euler angles of the grain. If one grid belongs to the p-th grain, $\eta_p=1$, η_q $(q\neq p)=0$, α_p $(\Phi_1,\Psi,\Phi_2)=(\alpha_p^{\Phi 1}=a, \alpha_p^{\Psi}=b, \alpha_p^{\Phi 2}=c)$, α_q $(\Phi_1,\Psi,\Phi_2)=(\alpha_q^{\Phi 1}=0, \alpha_q^{\Psi}=0, \alpha_q^{\Phi 2}=0\ (q\neq p))$, and the case is $\eta_p, \eta_q\in[0,1]$, η_i $(i\neq p,q)=0$, $\alpha_p(\Phi_1,\Psi,\Phi_2)=(\alpha_p^{\Phi 1}=a_1, \alpha_p^{\Psi}=b_1, \alpha_p^{\Phi 2}=c_1)$, $\alpha_q(\Phi_1,\Psi,\Phi_2)=(\alpha_q^{\Phi 1}=a_2, \alpha_q^{\Psi}=b_2, \alpha_q^{\Phi 2}=c_2\ (q\neq p))$, when the grid is in the GB area between grains marked as p and q. Moreover, the dihedral angle information can be deduced from the dihedral angle between α_p and α_q (see Subsection 2.2).

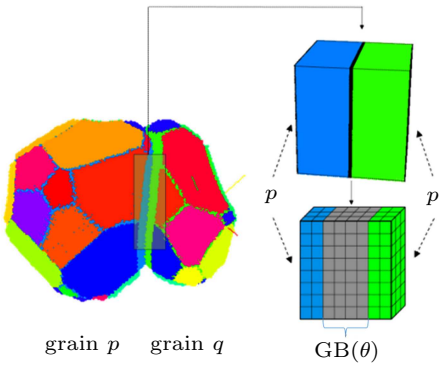


Fig. 1. Schematic diagram of GB between adjacent grains with different orientations, with gray area showing GB between grains p and q, and θ being dihedral angle between two grains.

For simplification, we only adopt order variables to describe the microstructure evolution in the ZK60 alloy, which is a single-phase polycrystalline system, according to Ref. [40]. Then the evolution can be described with the equations of non-conserved order variables based on the time-dependent

Ginzburg–Landau equation[41] given in the following,

$$\frac{\partial \eta_p(r,t)}{\partial t} = -L\frac{\delta F}{\delta \eta_p(r,t)}, \quad p = 1,2,3,\ldots n. \tag{1}$$

Here, L is a variable related to grain coarsening mobility and can be expressed in the form of Arrhenius law $L = L_0\,\mathrm{e}^{-Q/RT}$, where L_0 can be determined by calibrating the experimental results in ZK60 alloy, Q is thermal activity energy related GB movement, L is 16.8×10^{-3} mol/(J·s) according to our previous work,[38] and n is the number of grain orientations and it can be infinite to represent arbitrary grain orientation in real microstructure by adopting the APT algorithm[27,31] in our model.

The free energy can be expressed as follows:[38,40]

$$\begin{aligned} F &= \int_V f(\eta_1,\eta_2\ldots,\eta_p,\nabla\eta_1,\nabla\eta_2\ldots,\nabla\eta_p)\,\mathrm{d}V \\ &= \int_V \left[mf_0(\eta_1,\eta_2\ldots,\eta_p) + \frac{K_2}{2}\sum_{i=1}^{p}(\nabla\eta_i)^2\right]\mathrm{d}V, \end{aligned} \tag{2}$$

$$\begin{aligned} f_0 &= A - \frac{B_1}{2}\sum_{q=1}^{n}\eta_q^2(r,t) + \frac{B_2}{4}\sum_{q=1}^{n}\eta_q^4(r,t) \\ &\quad + \frac{K_1}{2}\sum_{q=1}^{n}\sum_{p\neq q}^{n}\eta_q^2(r,t)\,\eta_p^2(r,t). \end{aligned} \tag{3}$$

Inside a grain, m is a constant with a value of 1, $(K_2/2)\sum_{i=1}^{p}(\nabla\eta_i)^2 = 0$, $(K_1/2)\sum_{q=1}^{n}\sum_{p\neq q}^{n}\eta_q^2(r,t)\,\eta_p^2(r,t) = 0$, and f_0 is the free energy of ZK60 and can be obtained by THERMOCALC calculation. Hence, the related parameters A, B_1, and B_2 can be obtained by data fitting and quantitative relation. In the GB area, $m(\theta)$ and $K_2(\theta)$ are coefficients related to GB energy determined by the dihedral angle θ (see Subsection 2.3). We take $m = 1$, $K_1 = 2.05\times10^2$ J/mol, $K_2 = 4.4\times10^{-12}$ J·m^2/mol, $A = -26.3$ kJ/mol, $B_1 = 138.05$ J/mol, and $B_2 = 51.2$ J/mol for the uniform ZK60 alloy system at 573 K (For simplification, chemical composition is not considered in this model, the variable c in Ref. [38] is taken as a constant of 4.9%).

2.2. Dihedral angle between adjacent grains

Based on the Read–Shockley model, the GB energy is a function of dihedral angle between two neighboring gains. Meanwhile the dihedral angle is determined by the adjacent grains' orientations which are denoted in terms of Euler angles in our model.

The $\boldsymbol{g}_i$ and $\boldsymbol{g}_j$ are assumed to be adjacent grains' orientations expressed in terms of Euler angles, and $\boldsymbol{g}$ is the angular distance between $\boldsymbol{g}_i$ and $\boldsymbol{g}_j$. The angular distance between $\boldsymbol{g}_i$ and $\boldsymbol{g}_j$ is given as follows:

$$\boldsymbol{g}_i = \boldsymbol{g}_j\Delta\boldsymbol{g}. \tag{4}$$

Then, $\boldsymbol{g}$ can be expressed as follows:[42]

$$\begin{aligned} \Delta\boldsymbol{g} &= \boldsymbol{g}_i^{-1}\boldsymbol{g} = \left(-\varphi_2^i,-\phi^i,-\varphi_1^i\right)\left(\varphi_1^j,\phi^j,\varphi_2^j\right) \\ &= \left(\pi-\varphi_2^i,\phi^i,\pi-\varphi_1^i\right)\left(\varphi_1^j,\phi^j,\varphi_2^j\right) \\ &= \begin{bmatrix} \Delta g_{11} & \Delta g_{12} & \Delta g_{13} \\ \Delta g_{21} & \Delta g_{22} & \Delta g_{23} \\ \Delta g_{31} & \Delta g_{32} & \Delta g_{33} \end{bmatrix}. \end{aligned} \tag{5}$$

Meanwhile θ_{ij} and $\boldsymbol{g}$ satisfy the following function based on crystallographic spatial relations

$$1 + 2\cos\theta_{ij} = 1 + 2\cos|\Delta g| = \Delta g_{11} + \Delta g_{22} + \Delta g_{33}, \tag{6}$$

$$g = \begin{bmatrix} \cos\varphi_1\cos\varphi_2 - \sin\varphi_1\sin\varphi_2\cos\phi & \sin\varphi_1\cos\varphi_2 + \cos\varphi_1\sin\varphi_2\cos\phi & \sin\varphi_2\sin\phi \\ -\cos\varphi_1\sin\varphi_2 - \sin\varphi_1\cos\varphi_2\cos\phi & -\sin\varphi_1\sin\varphi_2 + \cos\varphi_1\cos\varphi_2\cos\phi & \cos\varphi_2\sin\phi \\ \sin\varphi_1\sin\phi & \cos\varphi_1\sin\phi & \cos\phi \end{bmatrix}. \tag{7}$$

Substitution of Eqs. (7) and (5) into Eq. (6) gives

$$\begin{aligned} \cos\frac{\theta_{ij}}{2} &= \cos\frac{(\varphi_1^i-\varphi_1^j\varphi_2^i-\varphi_2^j)}{2}\cos\frac{\phi_i}{2}\cos\frac{\phi_j}{2} \\ &\quad + \cos\frac{(\varphi_1^i-\varphi_1^j)-(\varphi_2^i-\varphi_2^j)}{2}\sin\frac{\phi_i}{2}\sin\frac{\phi_j}{2}. \end{aligned} \tag{8}$$

Finally, the angle (θ_{ij}) between g_i and g_j can be obtained as follows:

$$\begin{aligned} \theta_{ij} &= |\Delta\boldsymbol{g}| = \left|\boldsymbol{g}_i^{-1}\boldsymbol{g}\right| \\ &= 2\cos^{-1}\left[\cos\frac{(\varphi_1^i-\varphi_1^j)+(\varphi_2^i-\varphi_2^j)}{2}\cos\frac{\phi_i}{2}\cos\frac{\phi_j}{2}\right. \\ &\quad \left. + \cos\frac{(\varphi_1^i-\varphi_1^j)-(\varphi_2^i-\varphi_2^j)}{2}\sin\frac{\phi_i}{2}\sin\frac{\phi_j}{2}\right]. \end{aligned} \tag{9}$$

Thus, the dihedral angle of GB between arbitrary adjacent grains can be obtained based on real grain orientations according to Eq. (9). It should be noted that in order to simplify the model, equation (9) is applied to our model without considering the symmetry caused by special crystal structure. More derivation details are available in Ref. [42].

2.3. Anisotropy of GB energy in model

In this mode, the GB energy can be evaluated easily in the following way.[43] Equation (10) shows that the GB energy depends on the integral of local free energy density difference across the grain boundary area

$$\begin{aligned} \gamma_{i,j} &= \int_{-\infty}^{+\infty}\left\{m\Delta f_0(\eta_i,\eta_j)\right. \\ &\quad \left. + \frac{K_2}{2}\left[\left(\frac{\mathrm{d}\eta_i}{\mathrm{d}x}\right)^2 + \left(\frac{\mathrm{d}\eta_j}{\mathrm{d}x}\right)^2\right]\right\}\mathrm{d}x, \end{aligned} \tag{10}$$

where $\Delta f_0(\eta_i,\eta_j) = f_{0\,\mathrm{GB}} - f_{0\,\mathrm{matrix}}$, which means excess energy against matrix in the GB area.

According to the absolute value of the gradient based on the GB profile, Moelans *et al.*[40] derived the diffuse GB width in phase-field model, which shows that the GB width could remain unchanged with GB energy varied under the condition of a fixed ratio between K_2 and m. This research achievement makes it possible to establish a GB anisotropy model, which can characterize the microstructure including GBs with varying energy but fixed width, and K_2/m was taken as 4.4×10^{-12} in our target alloy system.[38]

The Read–Shockley model (R–S model), a GB energy model that takes into consideration the small dihedral angle between adjacent grains, has been introduced into the phase-field model.[26,44] We also adopt this model for investigating the anisotropic GB energy, and the conventional expression is as follows:

$$\begin{cases} E(\theta_{ij}) = 1.15\times\theta_{ij}\times\dfrac{\pi}{180}\times\left(0.31658-\ln\theta_{ij}\times\dfrac{\pi}{180}\right), & \theta_{ij}\le 20^\circ, \\ E(\theta_{ij}) = E_0, & \theta_{ij} > 20^\circ, \end{cases} \tag{11}$$

where E_0 is a constant proportional to the total density of dislocations, θ_{ij} is the dihedral angle of GB between adjacent grains (denoted as$i$ and j), and θ_m refers to the maximum dihedral angle for R–S model ($\theta_m = 20^\circ$). For $\theta_{ij} > 20^\circ$, $E(\theta_{ij})/E_0 = 1$ and in this model $E_0 = 0.55$ J/m^2, the same as the GB energy in a uniform system. The $E(\theta_{ij})$ has a range of $0\sim0.55$ J/m^2 in our model when $\theta_{ij}\le 20^\circ$. According to Eq. (10), the GB energy $E(\theta_{ij})$ depends on K_2 and m, and thus each of K_2 and m should also be a function of θ_{ij} in the GB area.

In order to determine the functional relationship between K_2 and θ, and between m and θ, the following steps are taken: (i) we first calculate the GB energy according to Eq. (10) (see Fig. 2(a)). (ii) Owing to lack of explicit relationship between GB energy and m, and between K_2 and m,[40] we employ a bicrystal model in a range of K_2 and m to calculate the GB energy value and implement a numerical fitting (see Fig. 2(b)). (iii) According to step (i) and step (ii), each GB energy correponds to a θ and a pair of K_2 and m, and functional relationships can be established by numerical fitting (see Fig. 2(c)). Thus, the relationship between model parameters (K_2 and m) and GB energy, which are both g related to θ, can be established based on the R–S model by means of numerical fitting. Finally, K_2 and m can be expressed as follows:

$$K_2(\theta) = 9.1998\times10^{-12}\times\theta\times\frac{\pi}{180}\times\left[0.31659-\ln\left(\theta\times\frac{\pi}{180}\right)\right], \tag{12a}$$

$$m(\theta) = 2.0925\times\theta\times\frac{\pi}{180}\times\left[0.31659-\ln(\theta\times\frac{\pi}{180})\right]. \tag{12b}$$

So far, the $m(\theta)$ and $K_2(\theta)$ can be determined by the real orientation information and GB energy in ZK60 alloy. The GB energy with an expression of continuous function based on real crystal orientations is determined in a 3D field model for the first time. In the textured system, the average GB energy and mobility are low because of a certain quantity of low-angle grain boundaries (LAGBs). The K_2 and m are taken as different values based on the dihedral angle of adjacent grains according to Eqs. (12a) and (12b). The procedures for searching and classificating GBs are summarized as follows.

(I) Check whether a grid has more than one η with a value less than a threshold (0.9 is taken in this model), if not, K_2 and m are taken as 4.4×10^{-12} J·m^2/mol and 1. In this situation, the grid is inside a grain.

(II) If there are two or more values of η larger than the threshold, the Euler angle $\alpha_i(\Phi_1,\Psi,\Phi_2)$ and $\alpha_j(\Phi_1,\Psi,\Phi_2)$ belonging to η_i and η_j, whose values are the first two largest values among all values of η, are extracted out and the dihedral angle θ_{ij} is calculated according to Eq. (9). This situation means that the grid is in a GB area.

(III) If $\theta_{ij} > 20$, it means that the GB type is high angle GB (HAGB), and K_2 and m are constants being the same as those in procedure (I).

If $0 < \theta_{ij}\le 20$, it means that the GB type is LAGB, and K_2 and m each are a function of θ_{ij} which can be calculated according to Eqs. 12(a) and 12(b).

If $\theta_{ij} = 0$, it means that the grains have the same orientation, namely, they are like grains. The η_j is set to be η_i. This means a coalescence of grains.

The coalescence will affect the grain growth process, and the APT algorithm, which can effectively avoid coalescing during grain growth, is adopted in this model.[27,31] A random orientation is assigned to each grain in the beginning, and it is possible that two grains have the same orientation, however, the probability is very low because the same orientation means that all 3 corresponding Euler angles are identical.

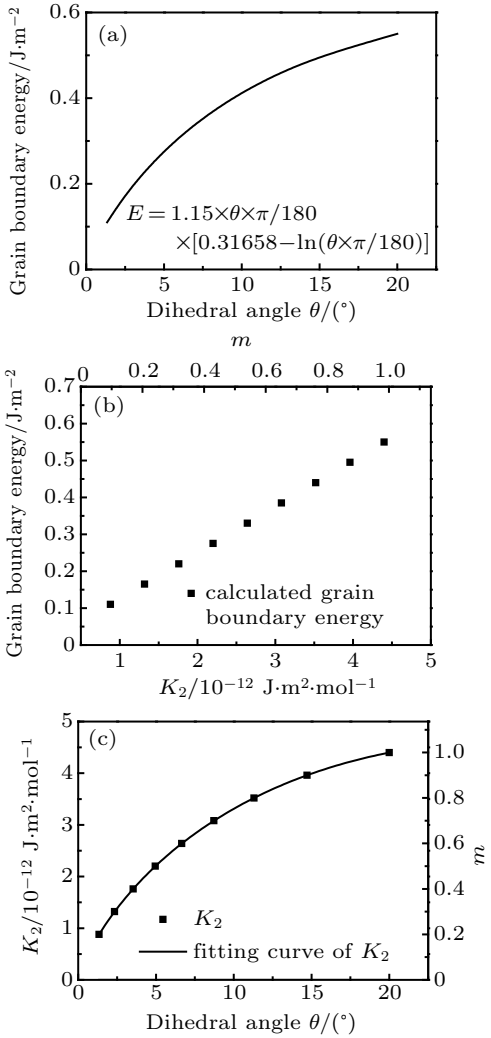


Fig. 2. (a) Curve of GB energy *versus* dihedral angle θ between grains based on R–S model; (b) relationship among K_2, m and GB energy based on bicrystal model (Fig. 1), (c) relationship among dihedral angle θ, K_2, and m, showing comparison between fitting curve and calculated values based on the data in panels (a) and (b).

2.4. Initial condition

The simulation is performed in a domain of $200\times200\times200$ grid points. In order to match the real microstructure in size, each grid point has a size of 0.293 μm and the GB range is about 1.172 μm which is the same as that in Ref. [38] because of the same model parameters. The time step t is taken as 0.18 s. We utilize a 16-node parallel computing message passing interface (MPI). In our model an APT algorithm is utilized so that we can realize each grain with an arbitrary orientation and an increase of computing effectiveness. Meanwhile a periodical boundary condition is chosen.

3. Results and discussion

3.1. System including 5 grains with different orientations

In order to perform a quantitative research of the effect of GB energy anisotropy on the grain evolution and test the validity as well as the accuracy of the model, a system including several grains with different orientations is built. For convenient comparison, a 5-grain system is set up as shown in Fig. 3(a). There are 5 grains inside a cubic lattice, 4 (marked as 1–4) of them form a sphere and the remaining part is grain 5. Euler angles of the 4 grains with the shape of quarter sphere are (0°, 5°, 0°), (0°, 8°, 0°), (0°, 13°, 0°), (0°, 20°, 0°), respectively. The rest of the cubic is matrix grain with an orientation of (0°, 0°, 0°). According to Refs. [45,46], the GB velocity follows the following equation:

$$v = M\gamma/R, \tag{13}$$

where M is the mobility coefficient of the GB and it is a constant in this system; γ is the GB energy depending on dihedral angle; R is the GB radius of curvature, and $1/R$ means GB curvature.

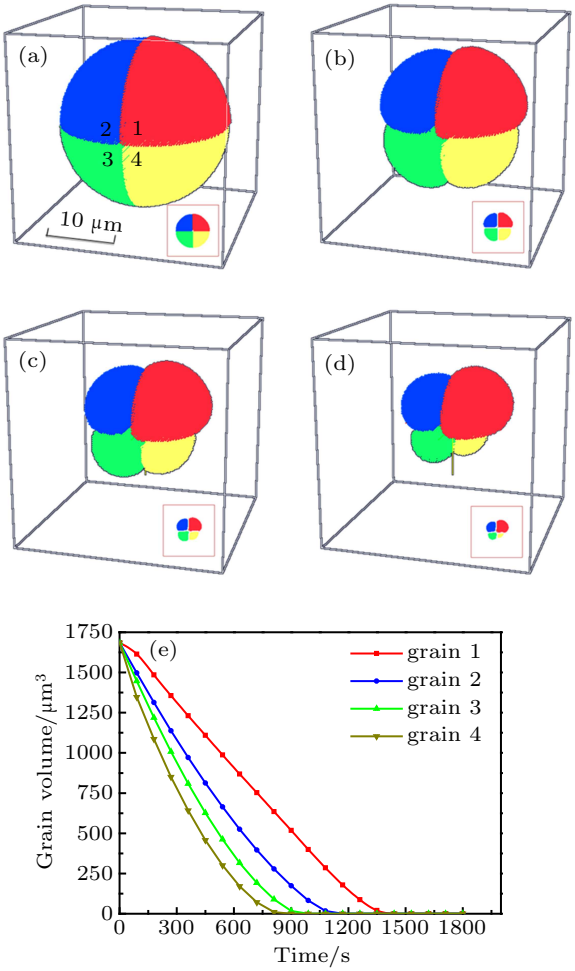


Fig. 3. Evolutions of grains with different orientations in 5-grain system. (a) Original state; after (b) 270 s, (c) 540 s, and (d) 720 s; (e) grain volumes varying with time for grains 1–4. Cubic cell includes 100^3 grids and each of grains 1–4 has 67020 grids in the beginning. Insets display sectional views showing that contacting GBs between grains 1–4 are mainly flat and mostly immobile during the evolution.

Grains 1–4 will shrink to minimize the GB energy of the system due to combined effects of the curvature and interfacial energy, and finally disappear. According to Eq. (13), the

velocity of GB movement depends on both curvature and GB energy. In the beginning, each of grains 1–4 has three faces, the one contacting matrix grain 5 is a curved GB and the other two are planes with a curvature of 0. Meanwhile grains 1–4 have the same shape initially and completely disappear finally, which means that the average curvature variations are roughly the same during evolution. Therefore, the shrinking velocities of grains 1–4 mainly depend on their GB energy with the matrix grain 5.

The initial shapes of grains 1–4 are set to have a radius of 11.72 μm. Figures 3(a)–3(d) show grains 1–4 evolve with time and the quantitative results are illustrated in Fig. 3(e). Simulation results show that the grain shrinkage becomes faster with the increase of GB energy caused by orientation difference between grains 1–4 and 5.

Meanwhile the average shrinking velocities can be calculated, and the ratio of velocities are 1:1.29:1.55:1.82, which accords well with the ratio (a value of 1:1.325:1.697:1.988) of GB energy between grains 1–4 and matrix grain 5. The difference mainly comes from the final process, when grain with high GB energy disappears and its neighboring grains change their shapes. Even so, the model can reflect the effect of GB energy anisotropy on grain growth effectively, and the quantitative comparative analysis indicates the validity and accuracy of the model.

3.2. Effect of GB energy anisotropy on evolution of polycrystalline system

The effect of GB energy anisotropy on a collective group grains' behavior is investigated, and the validated model is extended to a polycrystal system ofZK60 alloy. The GB type, depending on orientations of adjacent grains, changes with microstructure evolution. Therefore, it is impossible to accurately set up the proportion of GB with diverse types in a polycrystal system. However, it is convenient in this model to control the proportion of GB types, representing microstructures with different texture levels, within a certain appropriate range by setting up the number of grains in different orientation intervals. In this section, 5 kinds of microstructures with different levels of texture (listed in Table 1) are set up and we mainly study the effect of texture levels on dynamic and topological characteristics in ZK60 alloy.

Table 1. Microstructure conditions of different texture levels in our model.

Conditions	GB energy range	Grain orientation	Initial proportions of LAGB/%
1. Texture free	0.55 J/m^2	All GBs were treated as HAGBs.	0
2. Random texture	0–0.55 J/m^2	Each Euler angle of grains was assigned randomly.	6.13
3. Low texture		20% of grains orientation range was set in the range of (0°, 0° ∼ 20°, 0°), others were set randomly.	24.32
4. Medium texture		40% of grains orientation range was set in the range of (0°, 0° ∼ 20°, 0°), others were set randomly.	39.31
5. High texture		90% of grains orientation range was set in the range of (0°, 0° ∼ 20°, 0°), others were set randomly.	85.20

In conditions 3–5 in Table 1, we enhance the texture levels by increasing grains with an orientation in the range ($\Phi_1 = 0°$, $\Psi = 0 \sim 20°$, $\Phi_2 = 0°$), and the contacting probability of grains with similar orientations also increase. The LAGB ratio is calculated by dividing the overall GB area by LAGB area. Moreover, the real initial proportion of LAGB shows that higher proportion appeare in a higher textured microstructure. It should be noted that the main purpose of this study is to explore the influence of LAGB's proportion on the microstructure characteristics during evolution, thus the setting of grain orientations is effective and the CSL grain boundaries which are related to the lattice symmetry are ignored because of their less content in our simulation.

An initial polycrystalline microstructure is created by simulating grain growth for 500 steps as shown in Fig. 4, in a system with uniform GB energy (0.55 J/m^2). we use the same microstructure information shown in Fig. 4 (original column) as an initial grain structure for all simulations, including those with nonuniform GB energy in order to eliminate the effect of other influencing factors such as curvature, grain size, distribution, *etc*. The evolutions of microstructures with different texture levels (LAGB contents) are also shown in Fig. 4.

Microstructure evolvement is driven by an energy reduction in the way of consuming GB. In Fig. 4, all the microstructures are created under the same original condition, and thus it is easy to compare the evolving velocities of grains. It is obvious that at 1800 s most of grains in the texture-free system (see Fig. 4(a)) are larger than the grains obtained under other conditions, then they become the random and low textured systems which have similar initial LAGB content. Most of grains in the high textured system are smallest. It can be easily explained that adjacent grains have closer orientations in a higher textured system, which means more LAGBs and thus a slower average GB movement. The GB movement ve-

locity (v) can be expressed as the change of grain size with time, $\mathrm{d}R/\mathrm{d}t$. According to Eq. (13), $\mathrm{d}R/\mathrm{d}t = M\gamma/R$. Then the following equation can be obtained:

$$\overline{R}^2 - \overline{R}_0^2 = M\gamma t = kt. \tag{14}$$

The coefficient k in Eq. (14), which is mainly determined by the average GB energy in our system, is positively related to $\overline{R}^2$. Therefore, we predict that the GB energy can affect the grain growth kinetics, namely, the microstructure with more LAGBs can go through a slower evolution and obtain a smaller k in Eq. (14). Figure 5 shows the kinetic behavior of grain growth for a quantitative analysis in different systems.

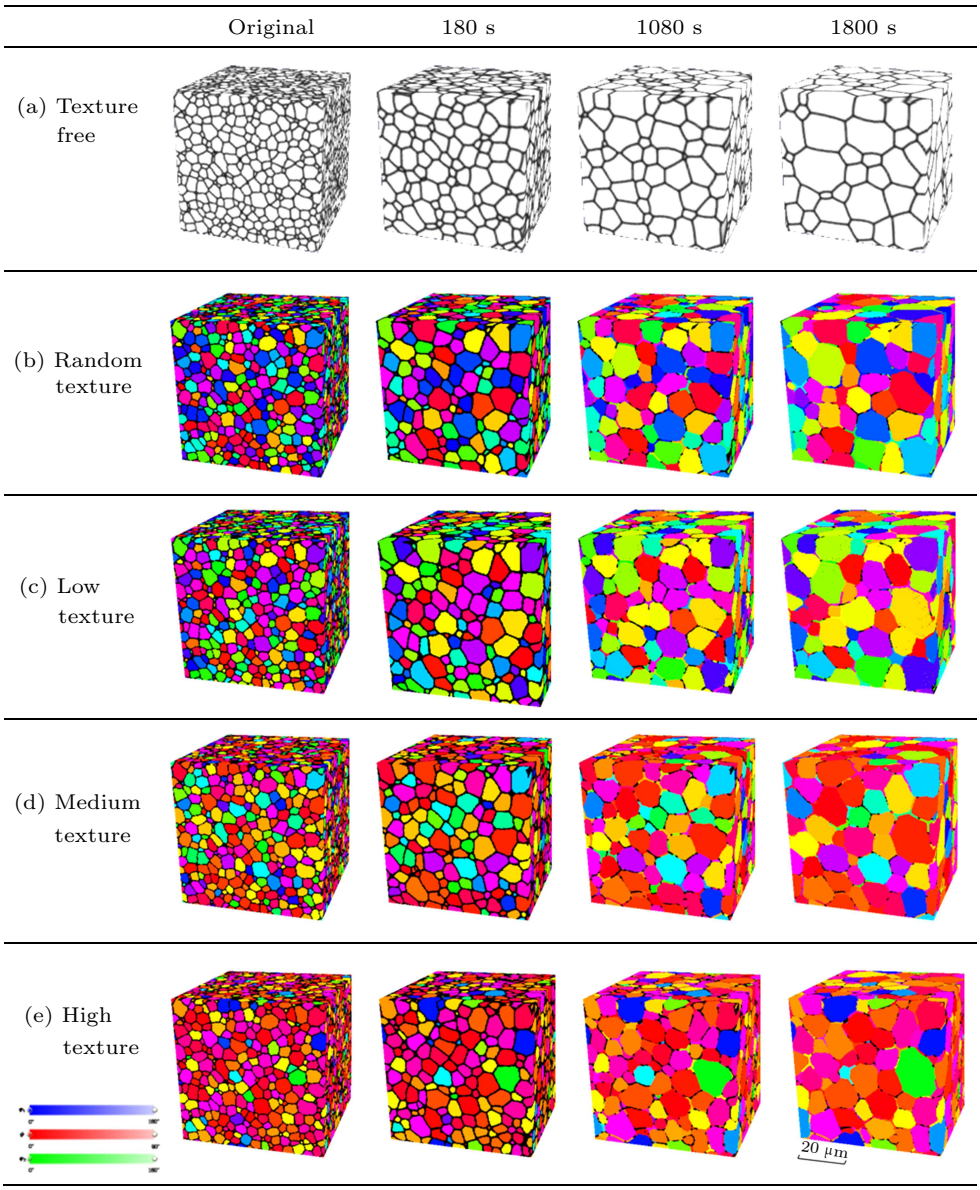


Fig. 4. Microstructure evolution with time under different conditions: (a) texture free; (b) random texture; (c) low texture; (d) medium texture; (e) high texture. There are 4545 grains in original microstructure, and there are 183, 214, 229, 273, and 383 grains in different microstructures at 1800 s.

Unsurprisingly, as our prediction, it can be seen that the GB energy has an obvious effect on the grain growth kinetics in Fig. 5. The speed of grain growth has an inverse relationship with the texture level, which means that in a polycrystalline system with a higher texture level (more small-angle GBs) can slow down the microstructure evolution. The results also show that they are in good agreement with the trends predicted by Mallick and Vedantam[27] and Miyoshi and Takaki in 2D simulation.[31]

Furthermore, we calculate the proportions of LAGB evolving with time, the results are shown in Fig. 6. It is shown that the proportions of LAGB are in different levels during microstructure evolution in the 5 systems. Meanwhile an interesting result is found that the proportion decreases first and increases later in the random and low textured system when the initial proportion is less than approximately 40%, while the value will decease with time in medium and high textured system when the initial proportion is not less than 40%. The

LAGBs have a slower moving velocity because of their lower GB energy, and they work in different ways during different evolving stages in low textured systems. Compared with the grains with more HAGBs, the grains with more LAGBs have slow growth velocities and thus a weak topological stability, which makes them easy to be consumed by their surrounding bigger grains in the beginning. The vanishing of small grains with LAGBs causes the LAGB proportion to decrease first. Then the rest of LAGBs mostly attach to more stable grains, and they will be kept and the HAGBs will disappear during grain growth at a faster speed because of their higher mobility, which causes the portion of LAGBs to increase later. Referring to the initial and finial proportions, it agrees well with the result in Ref. [37], which mainly discussed the situation in random and weakly-textured systems. In the medium and high textured system, more grains have similar orientations, and then grains with special orientation own more HAGBs and they will have a high growth speed if they are stable enough, and the adjacent grains with LAGBs will be consumed. Meanwhile new HAGBs can form with high probability because the grain with special orientations may easily meet the grain with common orientations after its adjacent grain has vanished. Therefore, the HGABs will increase with grain growth in a system with high texture level. It needs to be noted that although the LAGB proportions follow different trends in different systems, the average LAGB proportion increases with texture content increasing, and thus, higher texture system undergoes a slower evolvement (see Figs. 4 and 5).

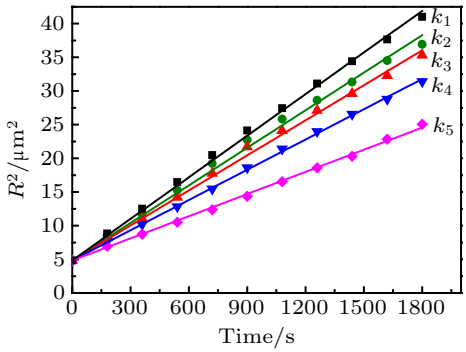


Fig. 5. Kinetic behaviors of grain growth in different systems. The values of k, obtained from fitting simulated data by least square method, are k_1 (texture free) = 0.0205 m^2/s, k_2 (random texture) = 0.0185 m^2/s, k_3 (low texture) = 0.0173 m^2/s, k_4 (medium texture) = 0.0149 m^2/s, and k_5 (high texture) = 0.0109 m^2/s respectively.

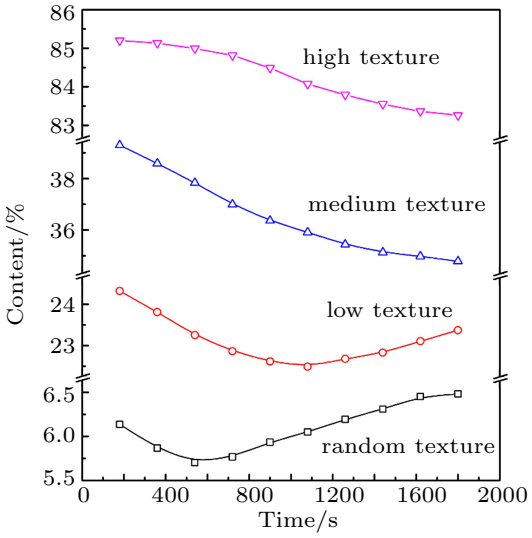


Fig. 6. Proportions of LAGB evolvement with time in different systems.

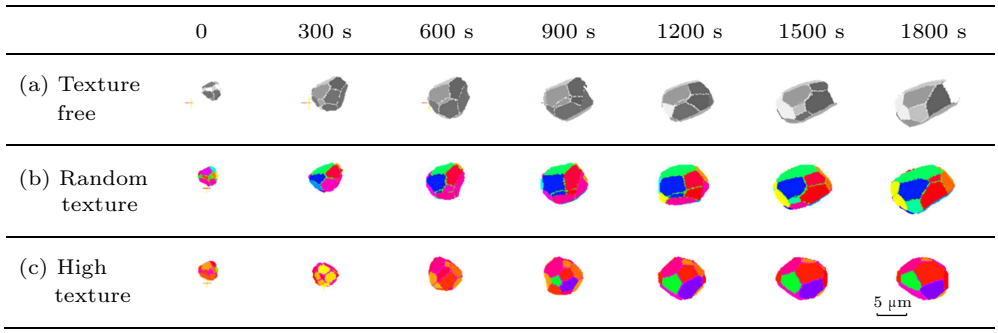


Fig. 7. Evolutions of grain with time under different conditions: (a) texture free, (b) random texture, and (c) high texture. Initial grains are the same, each with a size of 2.68 μm and 23 faces, and final sizes and faces are 6.4 μm, 19; 6.29 μm, 19; 5.58 μm, 18, respectively. Color bar is the same as that in Fig. 4.

The typical processes of single grain evolution in different systems are studied (see Fig. 7) for a close observation and the evidence of our previous conclusions. We choose the same grain in the initial microstructure, however, it has different surrounding conditions after the orientation assignments in the 3 systems (numbers 1, 2, and 5 in Table 1), and the surrounding conditions also vary during evolution. As a result, the grains go through different evolvement paths and the appearances of the grains are different from each other as shown in Fig. 7. Then a quantitative study on the kinetics and LAGB content of the grains is conducted (see Fig. 8). Figure 8 shows that the grain in a system with higher texture content grows slower, and the corresponding proportional range of LAGB follows the same trend. Furthermore, the variation of LAGB proportion during evolution in the 3 conditions are calculated and plotted in Fig. 8(b). In the uniform system, all the GBs are HAGB with energy of 0.55 J/m^2. In the other 2 systems, the LAGB proportions are shown in Fig. 8(b). It can be seen that

the LAGB around grain 2 varies in a range of 9%–12%, and LAGB around grain 3 varies in a range of 94%–95%. Combining with the results in Fig. 8(a), it can be concluded that the GB energy can affect the grain growth kinetics by influencing the GB movement in a polycrystal system.

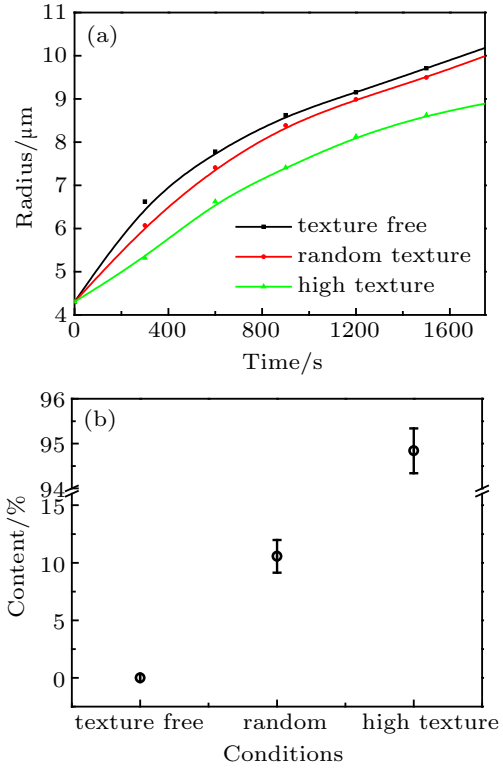


Fig. 8. (a) Kinetic features of single grain growth and (b) LAGB content of grain in different systems.

The topological characteristics such as size and face distributions are also discussed to study the effect of GB anisotropy on microstructures. For convenient comparison, the normalized grain size distributions at a particular time (1800 s) in different systems are plotted by data fitting as shown in Fig. 9(a). It can be seen that the distribution in the microstructure without texture has a peak at $R/R_{\rm ave} = 1$ and $R_{\rm max}/R_{\rm ave} = 1.85$, which is a typical feature of uniform system.[34,35] With the texture content increasing, the peaks are still at $R/R_{\rm ave} = 1$. However, their frequencies decrease and the curves become broader. Within a range of $1.4 > R/R_{\rm ave} > 0.7$, the frequency of grain decreases with texture content increasing. When the $R/R_{\rm ave}$ is less than 0.7 or more than 1.4, the frequency of grain increases with texture content increasing, which means that the grain size distribution becomes more concentrated around $R_{\rm ave}$ in a system with lower content of texture, and *vice versa*. As to the distribution of faces per grain, it is shown in Fig. 9(b) that in a uniform system an average is found to be 12.8 faces and this valueaccords well with previous result.[34,35] The frequency increases rapidly for a small number of faces and peaks at a value of 11, and then decays quickly, which is similar to that in Ref. [35]. With the increase of texture content, the distribution becomes broadened and follows the same trend as the distributions of grain sizes. Meanwhile, we also find that in the system with strong texture, there are more grains with faces less than 9 or more than 18 as indicated in Fig. 9(b).

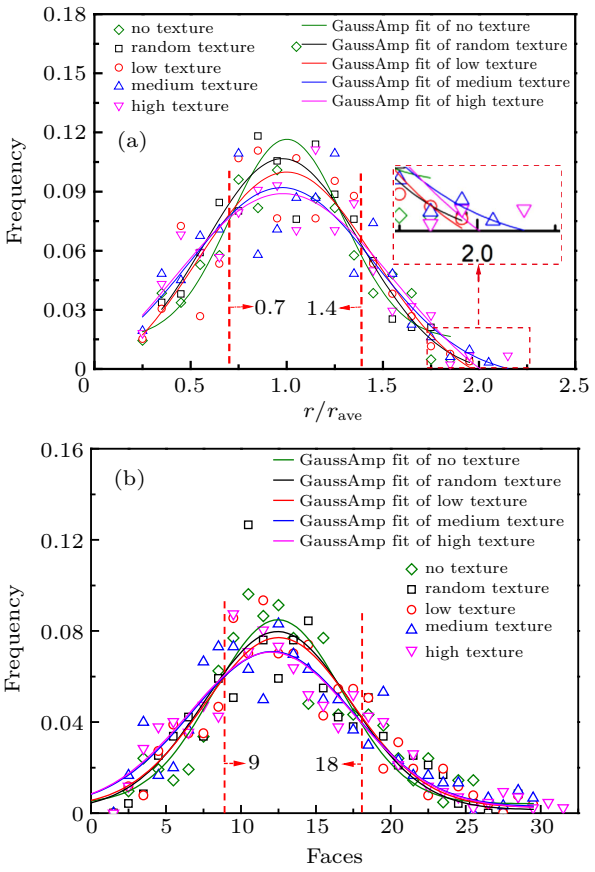


Fig. 9. Scaled distribution of (a) relative grain size ($R_{\rm ave}$ means averaged grain radius) and (b) faces per grain under different GB energy features, with data taken 1800 s before initial stages.

In order to describe this phenomenon quantitatively, a concept of relative grain size fluctuation is proposed. We define grain size fluctuation as the quotient of the difference between maximum and minimum 5% grain size and the average size as given as follows:.

$$\Delta d = \frac{d_{\rm max} - d_{\rm min}}{\bar{d}}. \tag{15}$$

In Fig. 10, the relative grain fluctuation varies with time and its values exhibit an increasing trend with texture content rising, which shows a good proof of our assumption. This means that the texture level will affect the fluctuation in grain size.

The reason could be that more grains have a similar orientation and LAGBs appear with a high probability in a system with a high texture level. On the one hand, this will result in a slower evolution (a smaller $R_{\rm ave}$ and $d_{\rm min}$), and on the other hand, some grains with special orientations which are quite different from those orientations of most grains, may

have more HAGBs and a higher expansion speed, which is the same reason as that discussed in Fig. 6. For example, a grain with a special orientation in a high textured system can easily own HAGBs by meeting grains with texture orientations. If the grain has a size advantage compared with its surrounding grains, it will grow up by consuming neighboring grains and have a greater opportunity to meet a grain with texture orientation, which can also cause another HAGB to form. Then, some special grains can evolve quickly and grain size fluctuation becomes more severe.

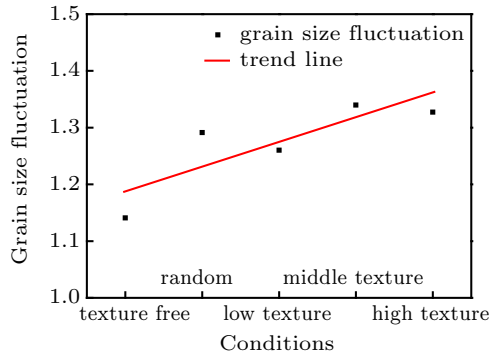


Fig. 10. Grain size fluctuation in different systems at 1800 s before initial stages.

A further analysis of data is carried out based on our simulated results to test this hypothesis. The volume ratios of non-textured grains in the 5% maximum group to all non-textured grains are calculated as shown in Fig. 11. The large grains contribute to the grain size fluctuation, and a higher ratio means that the non-textured grains with a volume advantage has a faster expansion. In Fig. 11, it can be seen that the ratio increases with texture level increasing, which confirms our hypothesis. Furthermore, all ratios in textured alloys are larger than the volume ratios of 5% maximum grains to all grains, whose values are between 19% and 21% in different systems with varying texture levels.

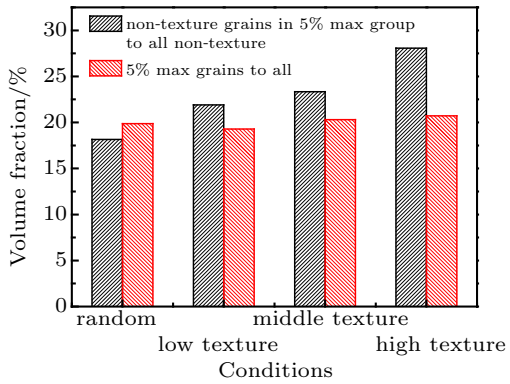


Fig. 11. Volume ratios of non-textured grains in the 5% max group to all non-textured grains in different systems, and ratios of 5% max grains to all.

In order to verify the results revealed by our simulation, a typical deformed ZK60 annealing structure is analyzed.[47] in Fig. 12. A higher texture level with a maximum intensity of 12.84 can be found in the microstructure. An analysis on the morphological features is carried out by a microstructure identification software developed by our team,[48] and the results are shown in Fig. 12(b). A serious fluctuation in grain size can be observed in Fig. 12(a), and the fluctuation value is 2.95 which is consistent with the observation. The areas (such as areas A and B) containing grains with similar orientations can be seen and the grain size is small because of lower GB mobility. Meanwhile some large grains with non-texture orientations, such as grain C and grain D, are also found. The volume ratio of non-textured grains in the 5% max group to all non-textured grains is 32.48% which is also in good agreement with our simulated result. Both the areas (such as areas A and B) with grains of similar orientations and the large grains with non-texture orientations contribute to a serious fluctuation in grain size according to our quantitative analysis. The analysis of the distribution of grain sizes also shows an uneven feature, which accords well with the morphological observation and our simulated result.

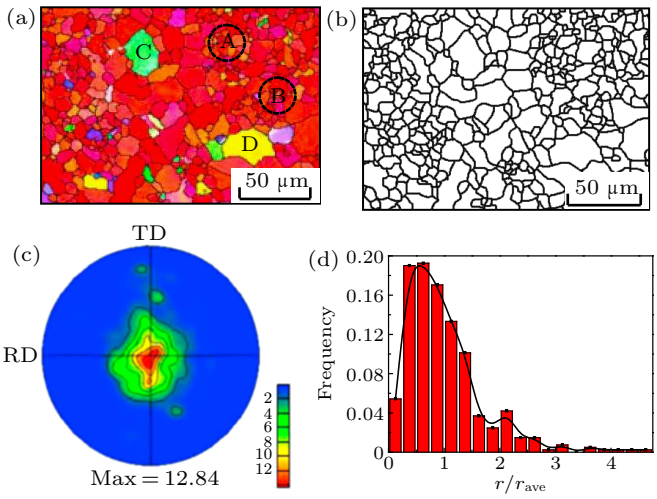


Fig. 12. (a) EBSD map of ZK60 Mg alloy,[47] (b) pole figure, (c) reconstitution map by software,[48] and (d) distribution of grain sizes.

The fluctuation in grain size describes the uniformity of microstructure. In a polycrystalline metal, the serious fluctuation in grain size means an uneven distribution of grains with different sizes. In general, a fluctuation in grain size has a strong effect on the mechanical properties such as tensile strength. In polycrystalline, the larger grains have lower resistance to plastic deformation and they will deform easily with a suitable orientation. The yield strength is badly influenced by these grains during the early stage of deformation and thus mechanical properties will become worse, which means that the serious fluctuation in grain size leads to low strength.[49,50] Based on our simulation results, the fluctuation in grain size will become more serious in a microstructure with a higher

texture level. Therefore, the fluctuation in grain size, which is harmful to mechanical properties of Mg alloys in most cases, can be lessened by reducing the texture level according to our results.

Above all, the GB movement velocities are all proportional to GB energy under the same GB curvature. A polycrystal system with high level texture, which means that more grains have similar orientations and more LAGBs exit, has a slow evolvement in an average grain size. Meanwhile some grains with special orientations evolve faster than others because they will most likely contact the grains of common orientation and HAGBs easily formed around them. Finally, the grain size fluctuation and topology will also be affected by he texture levels. Although our study is carried out in the ZK60 Mg alloy, the model can also be applied in other polycrystal alloy systems with proper parameters. The rules revealed by the simulation results should hold true in many polycrystal systems and are of great significance for uncovering how the GB anisotropy affects the evolution of polycrystalline during grain growth after being recrystallized.

4. Conclusions

In this study, a 3D polycrystal phase-field model with the GB energy anisotropy taken into consideration is built based on real grain orientations expressed as Euler angles, and the effect on the grain growth by GB energy anisotropy is studied in a ZK60 Mg alloy. The simulation results show that the GB energy anisotropy, normally caused by different texture levels, has effects on both kinetics and morphological features of microstructure. Also, the quantitative discussion and experimental proof are carried out. The conclusions are summarized below.

i) The GB energy anisotropy can cause the grain growth kinetics to change, namely, higher texture level, which also mean higher LAGB proportion, results in lower kinetics, and *vice versa*. In the ZK60 system, the kinetic index decreases from 0.0205 m^2/s to 0.0109 m^2/s with initial LAGB proportion varying from 5.69% to 89%.

ii) The LAGB proportion possesses different evolution characteristics in different texture level systems. The LAGB proportion first decreases and then increases in the random and low textured system, and the proportion decreases with time in the medium textured system and the high textured system.

iii) With the increase of texture content, the distribution of grain sizes, normalized by its average and faces per grain, becomes broader although the peak values are invariant, around $1(R/R_{\rm ave})$ and 11(faces per grain), respectively.

iv) The fluctuation in grain size increases with texture level becoming high, which accords well with the experimental observation. And the weakening of the texture level is an effective way of implementing a desired homogenized microstructure in ZK60 Mg alloy.

The phase-field model can be easily extended to other realistic alloy systems of single-phase polycrystalline with suitable model parameters, and the rules revealed in ZK60 alloy are applicable to other single-phase polycrystalline alloys due to the same mechanism of microstructure evolution. The rules revealed by the simulation results should be of great significance for uncovering how the GB anisotropy affects the temporal evolution of polycrystalline during grain growth after being recrystallized and offer ideas for processing alloy and optimizing microstructure.

References

[1] Lin J, Wang Q, Peng L and Roven H J 2009 *J. Alloys Compd.* **476** 441
[2] Hadadzadeh A, Wells M A, Shaha S K, Jahed H and Williams B W 2017 *J. Alloys Compd.* **702** 274
[3] Wang W, Cui G, Zhang W, Chen W and Wang E 2018 *Mater. Sci. Eng. A* **724** 486
[4] Wang W, Ma L, Chai S, Zhang W, Chen W, Feng Y and Cui G 2018 *Mater. Sci. Eng. A* **730** 162
[5] Bhattacharyya J J, Agnew S R and Muralidharan G 2015 *Acta Mater.* **86** 80
[6] Pérez-Prado M T and Ruano O A 2003 *Scr. Mater.* **48** 59
[7] Jamshidian M, Thamburaja P and Rabczuk T 2016 *J. Comput. Phys.* **327** 779
[8] Zhang T, Lu S H, Zhang J B, Li Z F, Chen P, Gong H and Wu Y X 2017 *Modell. Simul. Mater. Sci.* **25** 065005
[9] Tan Y, Maniatty A M, Zheng C and Wen J T 2017 *Modell. Simul. Mater. Sci.* **25** 065003
[10] Huo L, Han Z and Liu B 2009 *Acta Metall. Sin.* **45** 1414
[11] He R, Wang M, Jin J and Zong Y 2017 *Chin. Phys. B* **26** 128201
[12] Han G, Han Z, Luo A A and Liu B 2014 *Metall. Mater. Trans. A* **46** 948
[13] Han G, Han Z, Luo A A, Sachdev A K and Liu B 2013 *Scripta Mater.* **68** 691
[14] Zhang J, Teng C, Yang M, Xu D, Wang Y and Yang R 2013 *Chin. J. Nonferrous Met.* **23** 296
[15] Zhang J, Xu D, Wang Y and Yang R 2016 *Acta Metall. Sin.* **52** 905
[16] Han Z, Zhu W and Liu B 2009 *Acta Metall. Sin.* **45** 356
[17] Lewis R W, Han Z Q and Gethin D T 2007 *C. R. Mec.* **335** 287
[18] Moelans N, Blanpain B and Wollants P 2006 *Acta Mater.* **54** 1175
[19] Rehn V, H?tzer J, Rheinheimer W, Seiz M, Serr C and Nestler B 2019 *Acta Mater.* **174** 439
[20] Vedantam S and Patnaik B S 2006 *Phys. Rev. E* **73** 016703
[21] Kim D U, Cha P R, Kim S G, Kim W T, Cho J, Han H N, Lee H J and Kim J 2012 *Comput. Mater. Sci.* **56** 58
[22] Bhattacharyya S, Heo T W, Chang K and Chen L Q 2011 *Modell. Simul. Mater. Sci. Eng.* **19** 035002
[23] Shahnooshi E, Jamshidian M, Jafari M, Ziaei-Rad S and Rabczuk T 2019 *J. Cryst. Growth* **518** 18
[24] Suwa Y and Saito Y 2005 *Mater. Trans.* **46** 1208
[25] Abrivard G, Busso E P, Forest S and Appolaire B 2012 *Philos. Mag.* **92** 3643
[26] Asle Zaeem M, El Kadiri H, Wang P T and Horstemeyer M F 2011 *Comput. Mater. Sci.* **50** 2488
[27] Mallick A and Vedantam S 2009 *Comput. Mater. Sci.* **46** 21
[28] Miyoshi E and Takaki T 2016 *Comput. Mater. Sci.* **120** 77
[29] Steinbach I, Pezzolla F, Nestler B, SeeBelberg M, Prieler R, Schmitz G J and Rezende J L L 1996 *Physica D* **94** 135
[30] Steinbach I and Pezzolla F 1999 *Physica D* **134** 385
[31] Miyoshi E and Takaki T 2017 *J. Cryst. Growth* **474** 160
[32] Vuppuluri A and Vedantam S 2018 *J. Mater. Sci.* **54** 506

[33] McKenna I M, Gururajan M P and Voorhees P W 2009 *J. Mater. Sci.* **44** 2206
[34] Suwa Y, Saito Y and Onodera H 2007 *Comput. Mater. Sci.* **40** 40
[35] III C E K and Chen L Q 2002 *Acta Mater.* **50** 3057
[36] Chang K, Chen L Q, Krill C E and Moelans N 2017 *Comput. Mater. Sci.* **127** 67
[37] Kim H K, Kim S G, Dong W, Steinbach I and Lee B J 2014 *Modell. Simul. Mater. Sci. Eng.* **22** 034004
[38] Song Y, Wang M, Zong Y, He R and Jin J 2018 *Materials* **11** 1903
[39] Chen L Q 2002 *Ann. Rev. Mater. Res.* **32** 113
[40] Moelans N., Blanpain B.and Wollants P. 2008 *Phys. Rev. B.* **78** 024113
[41] Cahn J W 1961 *Acta Mater.* **9** 795
[42] Mao W and Zhang X 1993 *Quantitative Texture Analysis of Crystal Materials* (BeiJing: Metallurgical Industry Press) p. 235
[43] Zhang X, Zong Y, Wang M and Wu Y 2011 *Acta Phys. Sin.* **60** 068201 (in Chinese)
[44] Warren J A, Kobayashi R and Carter W C 2000 *J. Cryst. Growth* **211** 18
[45] Darvishi Kamachali R and Steinbach I 2012 *Acta Mater.* **60** 2719
[46] Burkeand J E and Turnbull D 1952 *Prog. Metal Phys.* **3** 220
[47] Song B, Xin R, Guo N, Xu J, Sun L and Liu Q 2015 *Mater. Sci. Eng. A* **639** 724
[48] Jin J, Li S, Cao J and An Y 2018SR02604 [2018-07-01]
[49] Liu G 1989 *Phys. Exam. Test.* **03** 26
[50] Park S H, Kim S H, Kim Y M and You B S 2015 *J. Alloys Compd.* **646** 932